

# Experimental and Theoretical Study of Photoenolization Mechanism for 1-Methylantraquinone

Nina P. Gritsan,\* Igor V. Khmelinski, and Oleg M. Usov

Contribution from the Institute of Chemical Kinetics and Combustion, 630090 Novosibirsk, USSR. Received July 31, 1990. Revised Manuscript Received April 8, 1991

**Abstract:** Photoenolization of 1-methylantraquinone (AQ) and its deuterated analogue (AQ- $d_6$ ) has been studied by laser flash photolysis over a wide temperature range (120–340 K). Phototransfer of a H (or D) atom has been found to occur in both the singlet and triplet  $n\pi^*$  states. The temperature dependence of the efficiency of the phototransfer of H and D atoms in the  $^1n\pi^*$  state has been analyzed. Piperylene quenching of AQ and AQ- $d_6$  triplet excited states has been studied. The rate constants of H- and D-atom phototransfer at room temperature have been estimated to be ca.  $3 \times 10^{10} \text{ s}^{-1}$  and ca.  $10^{10} \text{ s}^{-1}$ , respectively. Quantum-chemical calculations of potential energy surfaces and of electronic and geometrical structures of key intermediates have been performed by using the AM1 technique. A triplet  $\sigma,\pi$ -biradical has been found to be the intermediate preceding the formation of 9-hydroxy-1,10-antraquinone-1-methide (AQM). It has been revealed that thermal transformation of the enol AQM to the initial quinone AQ can occur as an intramolecular process via reverse transfer of a H atom, or as a second-order reaction. The latter appears to involve the transfer of two H (or D) atoms in a collisional complex of two AQM molecules. The dependence of the rate constants of the intramolecular thermal transfer of H and D atoms on temperature and solvent nature has been analyzed.

## Introduction

Most of the photochemical reactions of organic compounds are as a rule nonadiabatic processes. However, there are quite a large number of exceptions to this general rule.<sup>1</sup> Most known adiabatic reactions occur on the excited singlet surface of potential energy. Such processes are, for example, proton phototransfer via the hydrogen bond,<sup>2</sup> and weak complexation (excimer and exciplex formation).<sup>3</sup> These adiabatic processes result in anomalous fluorescent properties, such as the substantial Stokes shift of fluorescence spectra<sup>2</sup> or the luminescence of excited complexes.<sup>3</sup> Considerably less data have been reported on adiabatic photochemical reactions on the excited triplet energy surface. This is apparently associated with the fact that, in this case, it is very difficult to identify the adiabatic mechanism.<sup>1</sup>

Recent examples of adiabatic photoreactions via the triplet state are the acyl group phototransfer in 1-(acyloxy)antraquinone derivatives<sup>4</sup> and keto–enol tautomerism of 2-(2'-hydroxyphenyl)benzoxazole.<sup>5</sup> The most well-known triplet adiabatic (or by Turro's classification,<sup>1</sup> "pseudoadiabatic") reaction is the photoenolization of  $\alpha$ -alkylaryl ketones.<sup>6</sup> Photoenolization has been also described for  $\alpha$ -alkylquinones.<sup>7–9</sup> The triplet intermediate that precedes the formation of enol in the ground state is the excited triplet enol.<sup>6,9,10</sup>

Intramolecular proton transfer in the excited singlet state occurs usually at very high rate constants (ca.  $10^{12} \text{ s}^{-1}$ ) without activation

energies.<sup>2b,11</sup> The rate constant for hydrogen-atom transfer in the excited triplet state of  $\alpha$ -alkylaryl ketones has been estimated<sup>6c</sup> as ca.  $10^{10} \text{ s}^{-1}$ . There is no quantitative data on  $\alpha$ -alkylquinones. The aim of the present work was the detailed investigation of primary processes in the photoenolization of 1-methylantraquinone. We have considered the following questions:

(i) What are the roles of the singlet and triplet states in hydrogen and deuterium phototransfer?

(ii) Is the hydrogen and deuterium phototransfer a thermally activated process or may it be described as quantum tunnelling?<sup>12</sup>

(iii) What are the geometry and electronic structure of the triplet enol intermediate?

To answer these questions, we used not only experimental but also quantum-chemical methods that allowed us to determine the nature of the intermediates more definitively and to interpret experimental results.

## Experimental Section

**Apparatus.** To take the spectra of products unstable at room temperature, the samples were irradiated at 87 K (or at 77 K) in glassy matrices by the light of a high-pressure mercury lamp through a glass filter ( $240 \text{ nm} \leq \lambda \leq 400 \text{ nm}$ ). Absorption spectra were recorded on a Specord UV-vis spectrophotometer.

The description of the setup for laser flash photolysis has been given previously.<sup>13</sup> An excimer laser (10 ns, 10 mJ, 308 nm) was used for irradiation. The probing system consisted of a double prismatic monochromator, a probing high-pressure xenon lamp, and a photomultiplier. Signals were recorded on an analogue-to-digital converter (20 MHz, 8-bit, 1024 channels) connected to a minicomputer. Kinetic parameters were determined by the method of nonlinear least squares.<sup>14</sup> Sample temperature was varied within 120–350 K accurate to  $\pm 0.5 \text{ K}$  with a thermostabilized nitrogen stream. To vary oxygen concentration, an argon–oxygen mixture was bubbled through the solution for 20 min. Oxygen concentration was estimated from reported values of the Henry coefficient.<sup>15</sup>

**Synthesis of Reactants.** To obtain 1-methylantraquinone (AQ),  $\alpha$ -( $o$ -toluyl)benzoic acid and polyphosphoric acid were fused for 1 h at 180 °C and cooled, and water was added. Then the product was extracted by ether. The extract was passed through a thin  $\text{Al}_2\text{O}_3$  layer, concen-

(1) Turro, N. J.; McVey, J.; Ramamurthy, V.; Lechtken, P. *Angew. Chem., Int. Ed. Engl.* **1979**, *18*, 572.

(2) (a) Weller, A. *Naturwissenschaften* **1955**, *42*, 175. (b) Klopffer, W. *Adv. Photochem.* **1977**, *10*, 311. (c) Nagaoka, S.; Nagashima, U. *Chem. Phys.* **1989**, *136*, 153.

(3) (a) Förster, Th.; Kasper, K. Z. *Phys. Chem. (N.Y.)* **1954**, *1*, 275. (b) Walker, M. S.; Bednar, T. W.; Lumry, R. J. *Chem. Phys.* **1966**, *45*, 3455. (c) Birks, J. B. *Photophysics of Aromatic Molecules*; Wiley: London, 1970.

(4) (a) Gritsan, N. P.; Russkikh, S. A.; Klimenko, L. S.; Plyusnin, V. F. *Teor. Eksp. Khim.* **1983**, *19*, 455. (b) Gritsan, N. P.; Klimenko, L. S.; Shvartsberg, E. M.; Khmelinski, I. V.; Fokin, E. P. *J. Photochem. Photobiol., A* **1990**, *52*, 137.

(5) Grellmann, K. H.; Mordzinski, A.; Heinrich, A. *Chem. Phys.* **1989**, *136*, 201.

(6) (a) Small, D. R.; Scaiano, J. C. *J. Am. Chem. Soc.* **1977**, *99*, 7713. (b) Haag, R.; Wirz, J.; Wagner, P. J. *Helv. Chim. Acta* **1977**, *60*, 2595. (c) Kumar, C. V.; Chattopadhyay, S. K.; Das, K. P. *J. Am. Chem. Soc.* **1983**, *105*, 5143.

(7) Rommel, E.; Wirz, J. *Helv. Chim. Acta* **1977**, *60*, 38.

(8) (a) Gritsan, N. P.; Rogov, V. A.; Bazhin, N. M.; Russkikh, V. V.; Fokin, E. P. *Teor. Eksp. Khim.* **1979**, *15*, 290. (b) Gritsan, N. P.; Bazhin, N. M. *Izv. Sib. Otd. Akad. Nauk SSSR* **1979**, 138. (c) Gritsan, N. P.; Shvartsberg, E. M.; Khmelinski, I. V.; Russkikh, V. V. *Zh. Fiz. Khim.* **1990**, *64*, 3081.

(9) Grummt, U.-V.; Friedrich, M. Z. *Chem.* **1985**, 434.

(10) Wirz, J. *Pure Appl. Chem.* **1984**, *56*, 1289.

(11) (a) Laermer, F.; Elsaesser, T.; Kaiser, W. *Chem. Phys. Lett.* **1988**, *148*, 119. (b) Dick, B.; Ernsting, N. P. *J. Phys. Chem.* **1987**, *91*, 4261.

(12) Formosinho, S. J. *Chem. Soc., Faraday Trans. 2* **1974**, *70*, 605; **1976**, *72*, 1313.

(13) Grivin, V. P.; Khmelinski, I. V.; Plyusnin, V. F.; Blinov, I. I.; Balashev, K. P. *J. Photochem. Photobiol., A* **1990**, *51*, 167.

(14) Johnson, K. J. *Numerical Methods in Chemistry*; Dekker: New York, 1983.

(15) Kogan, V. B.; Fridman, V. M.; Kafarov, V. V. *Reference Book on Solubility*; Izd-vo AN SSSR: Moscow, 1961; Vol. 2, p 22.

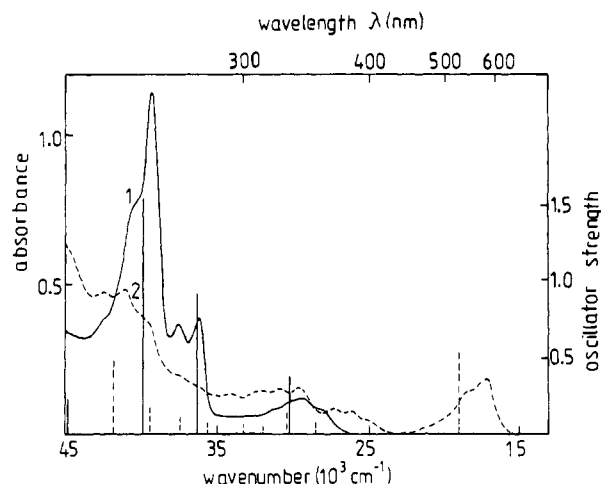


**Figure 1.** Absorption spectra of 1-methylanthraquinone (1) and the product of its photolysis (2) in ethanol at 87 K. Vertical lines indicate positions of absorption band maxima and oscillator strengths of transitions in the absorption spectra of 1-methylanthraquinone (solid lines) and 9-hydroxy-1,10-anthraquinone-1-methide (dashed lines), calculated by the PPP method.

trated by evaporation, and double sublimated at a pressure of 17 Torr ( $T_{\text{melt}} = 171.5^\circ\text{C}$ ).

1-(Trideuteriomethyl)-2,3,4-trideuterioanthraquinone (AQ- $d_6$ ) was obtained from toluene- $d_8$ , which was brominated in the presence of  $\text{FeBr}_3$ . Solid *p*-bromotoluene was separated by freezing out, and the residue was distilled in vacuo. Then *o*-bromotoluene- $d_7$  was used to obtain the corresponding deuterated toluylbenzoic acid by the Grignard synthesis. Further procedures are similar to those employed in the case of AQ.

**Solvent Purification.** Before being used, the solvents were purified as described.<sup>16</sup> Hexane, toluene, and ether were dried by melted  $\text{CaCl}_2$  and metallic sodium and then distilled over metallic sodium. Tetrahydrofuran was shaken with concentrated KOH solution, washed with water, and then dried as before. Ethyl acetate was stored for 3 days over annealed potash and then distilled over  $\text{P}_2\text{O}_5$ . Acetonitrile was boiled and distilled three times over  $\text{P}_2\text{O}_5$  for 6 h, and a fourth time over anhydrous potash. Ethanol was purified as described elsewhere:<sup>17</sup> boiled with NaOH and distilled. To obtain the absolute solvents, methanol and ethanol were boiled with Mg activated by iodine and distilled.

Deuteriomethanol and deuterioethanol from Izotop were used without further purification. Piperylene used as a quencher was distilled.

### Calculation Details

Quantum-chemical calculations of the electronic structure, potential energy surfaces, and geometry of AQ and 9-hydroxy-1,10-anthraquinone-1-methide (AQM) in the ground and lowest excited triplet states were performed by using the AM1 technique<sup>18</sup> on the MNDO-85 modified program.<sup>19</sup> The standard Davidson-Fletcher-Powell procedure<sup>20</sup> was used for optimization of the geometry. Singlet-singlet and triplet-triplet absorption spectra were calculated by using the CNDO technique<sup>21</sup> on Maslov's program.<sup>22</sup> Other calculations of absorption spectra were performed by the Pariser-Parr-Pople (PPP) method with the "variable  $\beta$ " approximation.<sup>23</sup> Properties of open-shell systems were calculated by using a method similar to the "half-electron" one.<sup>24</sup>

(16) Weissberger, A.; Proskauer, E. S.; Riddick, J. A.; Toops, E. E. *Organic Solvents. Physical Properties and Methods of Purification*; Interscience: New York, 1955.

(17) Parker, C. A. *Photoluminescence of Solutions*; Elsevier: Amsterdam, 1968.

(18) Dewar, M. J. S.; Zebisch, E. G.; Healy, E. F.; Stewart, J. J. J. *Am. Chem. Soc.* **1985**, *107*, 3902.

(19) Bliznyuk, A. A.; Voityuk, A. A. *Zh. Strukt. Khim.* **1986**, *27*, 190.

(20) (a) Fletcher, R.; Powell, M. J. D. *Comput. J.* **1963**, *6*, 163. (b) Davidson, W. C. *Comput. J.* **1968**, *10*, 406.

(21) Del Bene, J.; Jaffe, H. H. *J. Chem. Phys.* **1968**, *48*, 1807.

(22) (a) Maslov, V. G. *Zh. Strukt. Khim.* **1977**, *18*, 414. (b) Data of the Bank of Quantum-Chemical Programs; Inst. of Chemical Kinetics and Combustion (SFKP-58), Novosibirsk **1989**, *3*, 24.

(23) Nishimoto, K.; Forster, L. S. *Theor. Chim. Acta* **1965**, *3*, 407; **1966**, *4*, 155.

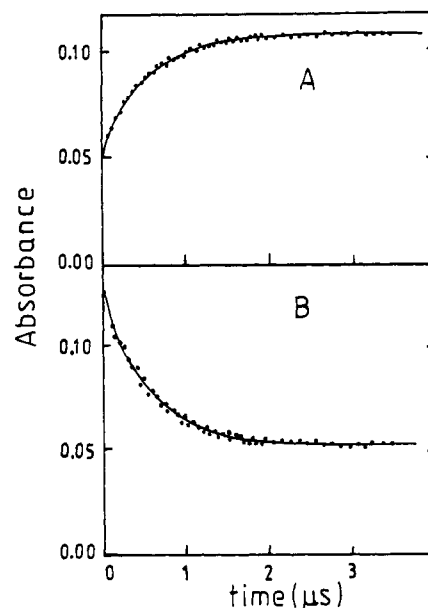


**Figure 2.** Kinetics of absorption increase at 580 nm (A) and decay at 380 nm (B), after pulse excitation of 1-methylanthraquinone in ethanol at 206 K without oxygen. Solid curves represent fitting by exponential time dependence ( $k = 1.85 \times 10^6 \text{ s}^{-1}$ ).

### Results and Discussion

**Low-Temperature Photolysis.** It has been shown<sup>8</sup> that irradiation of AQ and some of its derivatives in alcohol matrices at 77 K (or 87 K) results in hydrogen-atom transfer and formation of the corresponding 9-hydroxy-1,10-anthraquinone-1-methide (AQM).

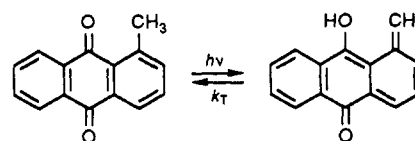


Figure 1 shows the change in the spectrum of AQ during long-duration irradiation, and the theoretical spectra of AQ and AQM calculated by the PPP technique.<sup>23</sup> It is seen that the calculated spectrum of AQM satisfactorily describes the spectrum of the photolysis product. AQM is stable in an alcohol matrix at temperatures lower than 120 K both in the dark and under long-duration irradiation. The structure of initial AQ is recovered only when the sample is heated to a temperature of above 120 K. In hydrocarbon matrices, AQM is unstable even at 77 K. The quantum yield of AQ photolysis at 77 K in ethanol is equal to 0.2. The presence of donor substitutes in the anthraquinone nucleus, e.g. piperidyl in position 4, leads to a substantial decrease in the quantum yield and its dependence on radiation wavelength<sup>8b</sup> ( $\phi_{334} = 1.4 \times 10^{-3}$ ,  $\phi_{436} = 10^{-4}$ ).

On the basis of such dependence and the correspondence of the AQ spectrum with that of anthraquinone, we have concluded previously<sup>8b</sup> that the reactive state has the  $\pi\pi^*$  configuration. Indeed, it is well known<sup>12,25</sup> that  $\pi\pi^*$  states are active in the reaction of hydrogen abstraction. Below we shall consider only results obtained for AQ and its deuterio derivative AQ- $d_6$ . The quantum yield for the photolysis of AQ- $d_6$  at 77 K is 0.4.

**Flash Photolysis of AQ and AQ- $d_6$ .** When exciting AQ in all studied solvents, we detected an accumulation of AQM in the ground singlet state and its decay. The decay of AQM absorption is caused by the recovery of the initial compound, AQ, and will

(24) (a) Longuet-Higgins, H. C.; Pople, J. A. *Proc. Phys. Soc., London* **1955**, *A68*, 591. (b) Dewar, M. J.; Hashmall, J. A.; Venier, C. G. *J. Am. Chem. Soc.* **1968**, *90*, 153. (c) Voityuk, A. A. *Zh. Strukt. Khim.* **1983**, *24*, 18.

(25) (a) Dauben, W. G.; Salem, L.; Turro, N. J. *Acc. Chem. Res.* **1975**, *8*, 42. (b) Suppan, P. J. *Chem. Soc., Faraday Trans. 2* **1986**, *82*, 2167.

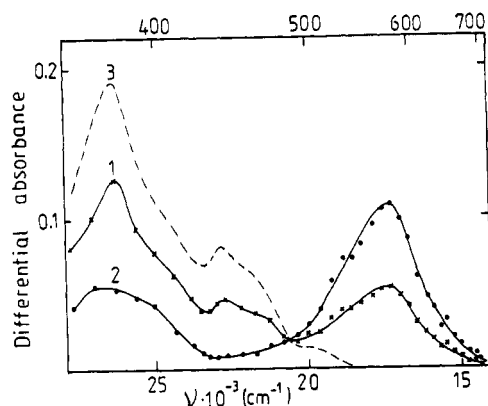


**Figure 3.** Differential absorption spectrum detected immediately after pulse excitation of 1-methylantraquinone (1), the absorption spectrum of 9-hydroxy-1,10-anthraquinone-1-methide detected 3.5  $\mu$ s after laser pulse (2), and the absorption spectrum of the triplet intermediate (T) estimated by the formula  $D(T) = 1.96 D(0) - 0.96 D(3.5 \mu s)$ , in ethanol at 206 K.

be discussed in detail below. At 206 K the AQM decay occurs in times considerably longer than the decay time of the AQM accumulation from the precursor. Hence, in the analysis of the accumulation kinetic curve, the decay may be ignored (Figure 2). At higher temperatures, the absorption kinetics were analyzed on the assumption that both AQM formation and decay are described by a first-order reaction.

It can be seen from Figure 3 that immediately after laser flash for wavelengths  $\lambda \geq 500$  nm absorption is observed, giving a spectrum practically coinciding with that of AQM. Earlier this absorption was assigned to the spectrum of the precursor.<sup>9</sup> Within 550–700 nm at 206 K the ratio of the optical density in zero time to the optical density in 3.5  $\mu$ s equals  $0.49 \pm 0.02$ . This value depends on temperature and particularly on AQ deuteration. For AQ this dependence is rather weak: the value changes from 0.55 at 298 K to 0.47 at 120 K. For AQ- $d_6$  it changes significantly: from 0.43 at 320 K to 0.12 at 120 K (accurate to  $\pm 0.02$ ). This result can be accounted for by assuming that the absorption after laser flash in the range 550–700 nm also corresponds to AQM in the ground state, formed from the excited singlet AQ state ( $^1n\pi^*$ ). In a wide temperature range (120–300 K), the total quantum yield is independent of temperature and deuteration and equals unity (accurate to  $\pm 10\%$ ). Hence, the ratio of AQM absorption at zero time to the limiting value of AQM absorption coincides with the absolute quantum yield of AQM formation from the  $^1n\pi^*$  state. The difference of this quantum yield from unity is due to competition of the phototransfer with rate constant  $k_t^s$  and intersystem crossing with rate constant  $k_d^s$ . The quantum yield is  $\varphi = k_t^s / (k_t^s + k_d^s)$ . Knowing  $\varphi$ , we can estimate the constant ratio by the formula

$$k_t^s / k_d^s = \varphi / (1 - \varphi) \quad (1)$$

It is seen (Figure 4) that for AQ the constant ratio becomes temperature independent at  $T \leq 200$  K, and the phototransfer of H atom in the  $^1n\pi^*$  state can be treated as quantum tunnelling.<sup>12</sup> Intersystem-crossing rate constants for carbonyl compounds are known to be very high<sup>26</sup> (e.g. for benzophenone<sup>26b</sup>  $k_d^s = 1.2 \times 10^{11} \text{ s}^{-1}$ ). Consequently, the rate constant of hydrogen-atom tunnelling is close to the rate constant of intersystem crossing and equals ca.  $10^{11} \text{ s}^{-1}$ . Unlike the hydrogen-atom phototransfer, that of deuterium in the singlet state is activated all over the temperature range under study (350–120 K). The activation energy is not very high,  $2.5 \pm 0.1 \text{ kJ/mol}$ .

**AQM Formation from the Triplet Precursor.** The kinetic curve shown in Figure 2 corresponds to AQM accumulation from the precursor in the absence of oxygen. With oxygen present, the

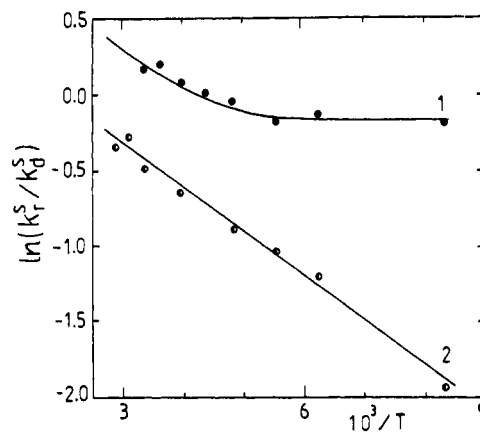


**Figure 4.** Temperature dependence of the ratio of the phototransfer rate constant ( $k_t^s$ ) of hydrogen (1) or deuterium (2) atom in the excited singlet state of 1-methylantraquinone to the rate constant of intersystem crossing from this state ( $k_d^s$ ).

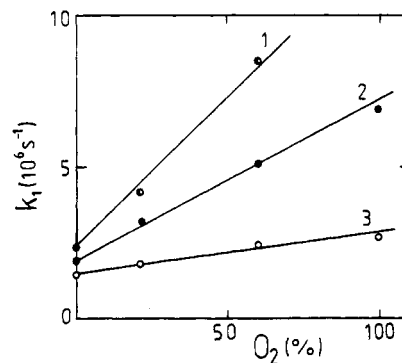


**Figure 5.** Rate constant of 9-hydroxy-1,10-anthraquinone-1-methide formation in ethanol at 251 K (1), 206 K (2), and 160 K (3) vs oxygen content of the gas mixture bubbled through the solution.

pseudo-first-order rate constant,  $k_1$ , is linear with concentration of dissolved  $O_2$  (Figure 5) and can be expressed in the form:

$$k_1 = k_1^0 + k_q[O_2] \quad (2)$$

where  $k_1^0$  and  $k_q$  are temperature-dependent values (Figure 5). Although  $k_1$  increases substantially with dissolved oxygen concentration, AQM yield in this case is independent of oxygen concentration and remains equal to unity (accurate to  $\pm 10\%$ ). The precursor of AQM as well as of enol in the case of *o*-alkylaryl ketones is an excited triplet species, T. The absorption spectrum of T is given in Figure 3 (curve 3). The T lifetime at 120 K in ethanol is 1.1  $\mu$ s and 1.4  $\mu$ s for AQM and AQM- $d_6$ , respectively. Oxygen quenching of the excited triplet states is a well-known process.<sup>3c,27</sup> It may be caused not only by energy transfer but also by increased intersystem crossing<sup>28</sup> in the presence of  $O_2$ . The rate-constant value for oxygen quenching at 251 K as estimated from the oxygen solubility<sup>15</sup> (0.0082 mol/L-atm) is ca. 40% of the diffusion-limited value and equals  $1.2 \times 10^9 \text{ L/mol}\cdot\text{s}$ .

**The Influence of Piperylene Admixtures on Quantum Yield.** Piperylene admixtures have no effect on the constant  $k_1^0$  and lead to an appreciable decrease in AQM quantum yield. The intermediate absorption in zero time is independent of piperylene admixtures. Figure 6 shows a Stern–Volmer plot for quenching the yield of AQM formed from the triplet precursor. It is seen

$$\varphi_T^0 / \varphi_T - 1 = K_Q[Q] \quad (3)$$

that the quantum yield is substantially affected only by very high concentrations of the quencher ( $\geq 1 \text{ M}$ ). Theoretically, such high concentrations allow not only diffusion-controlled dynamic

(26) (a) Plotnikov, V. G. *Usp. Khim.* **1980**, *49*, 327. (b) Borisevich, N. A.; Lysak, N. A.; Melnichuk, S. V.; Tikhomirov, S. A.; Tolstozheev, G. B. *Dokl. Akad. Nauk SSSR* **1987**, *295*, 900.

(27) Cijezman, O. L. J.; Kaufman, F.; Porter, G. J. *Chem. Soc., Faraday Trans. 2* **1973**, *69*, 708.

(28) (a) Smith, G. J. J. *Chem. Soc., Faraday Trans. 2* **1982**, *78*, 769. (b) Gorman, A. A.; Hamblett, I.; Rodgers, M. A. J. *J. Photochem.* **1984**, *25*, 115.

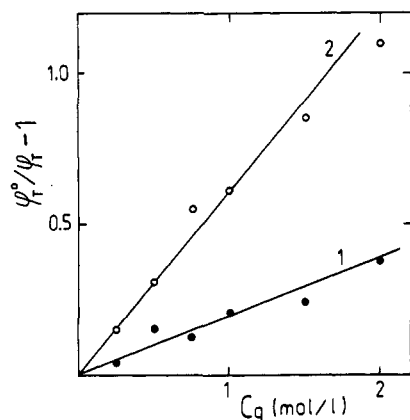


**Figure 6.** Stern-Volmer plots for piperylene quenching of the excited triplet state of 1-methylanthraquinone (1) and its deuterated analogue (2) ( $7.5 \times 10^{-4}$  M in ethanol at 298 K).

**Table I.** Stern-Volmer Constants for Quenching of the Excited Triplet States of 1-Methylanthraquinone ( $K_Q^H$ ) and its Deuterio Derivative ( $K_Q^D$ ), and H ( $k_H^T$ ) and D ( $k_D^T$ ) Atom Transfer Rate Constants<sup>a</sup>

T, K	$K_Q^H$ , L/mol	$K_Q^D$ , L/mol	$k_H^T$ , s <sup>-1</sup>	$k_D^T$ , s <sup>-1</sup>
298	0.20	0.60	$2.9 \times 10^{10}$	$10^{10}$
206	0.27	0.87	$1.5 \times 10^9$	$4.8 \times 10^8$

<sup>a</sup> Accuracy,  $\pm 20\%$ .

quenching but also static quenching in a complex. Therefore, generally speaking, measurements on high-concentration quenching can yield only the upper estimate of the excited-state lifetime. However, the significant difference in Stern-Volmer constants ( $K_Q$ ) for AQ and AQ- $d_6$  (Table I), as well as the absence of some changes in the absorption spectrum of AQ with adding piperylene up to 2 M, points to the dynamic character of the piperylene quenching of the triplet excitation of AQ. The  $^3n\pi^*$ -state lifetimes for AQ and AQ- $d_6$  were estimated on the assumption that the quenching is a diffusion-controlled process. As the photolysis quantum yield equals unity, H- and D-phototransfer rate constants are equal to the reciprocal lifetime of  $^3n\pi^*$ . The phototransfer rate constants (Table I) are seen to be high and temperature dependent. The kinetic isotope effect  $k_H^T/k_D^T$  is  $3.0 \pm 0.1$  and is independent of temperature (for 298 and 206 K). Hence, at least at temperatures higher than 200 K, the phototransfer of hydrogen and deuterium atoms in the excited triplet  $n\pi^*$  state is thermally activated.

**Properties of the Intermediate T.** It is seen from Figure 5 that the lifetime of the triplet intermediate in the absence of the quencher is temperature dependent. Moreover, the T lifetime depends on deuteration. The temperature dependence of the deactivation rate constant for T in the absence of oxygen (Figure 7) is satisfactorily described by the equation

$$k_1^0 = k^0 + k' \exp(-E/RT) \quad (4)$$

where  $k^0$ , within the accuracy of the experiment, is the same for AQ and AQ- $d_6$  (Table II). The kinetic isotope effect,  $k_1^0(\text{H})/k_1^0(\text{D})$ , turned out to be connected primarily with the deuteration dependence of the second term of expression 4, and grew with temperature from  $1.3 \pm 0.2$  at 120 K to  $2.6 \pm 0.5$  at 298 K. The kinetic isotope effect at room temperature has been estimated<sup>9</sup> to equal  $4.1 \pm 0.6$ .

Figure 7 also shows results obtained for AQ- $d_6$  in nondeuterated ethanol. As seen in this case, at high temperatures ( $\geq 250$  K) the deactivation rate constant is the same as that for nondeuterated T, and with decreasing temperature it approaches the rate constant for a deuterated sample in deuterioethanol. Consequently, at temperatures higher than 250 K, the reaction of the exchange of the deuterium of the OD group of T for the hydrogen of the alcohol OH group proceeds much faster than the deactivation of T. At 160 K the deactivation appears to run faster than the exchange reaction. Besides, T lifetime depends only on deuteration

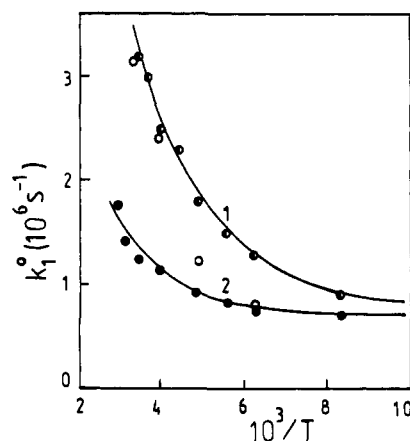


**Figure 7.** Temperature dependence of formation rate constant of 9-hydroxy-1,10-anthraquinone-1-methide from the triplet precursor in the absence of oxygen in ethanol (1) and its deuterated analogue in deuterioethanol (2) and ethanol (open circles). Solid lines indicate fitting by eq 4.

**Table II.**  $k_0$ ,  $k'$ , and  $E$  Values Determined from Fitting of Temperature Dependence of Deactivation Rate Constant of T by the Formula  $k_1^0 = k_0 + k' \exp(-E/RT)$

compd	solvent	$k_0$ , s <sup>-1</sup>	$k'$ , s <sup>-1</sup>	$E$ , kJ/mol
AQ	C <sub>2</sub> H <sub>5</sub> OH	$(7.5 \pm 0.7) \times 10^5$	$(1.6 \pm 0.3) \times 10^7$	$4.5 \pm 0.5$
AQ- $d_6$	C <sub>2</sub> H <sub>5</sub> OD	$(7.1 \pm 0.5) \times 10^5$	$(9 \pm 3) \times 10^6$	$6.4 \pm 1.3$

**Table III.** Dependence of T Lifetime ( $\tau$ , ns) on Solvent Nature at 206 K

compd	solvent		
	hexane	toluene	ethanol
AQ	$250 \pm 50$	$280 \pm 20$	$560 \pm 30$
AQ- $d_6$	$500 \pm 50$	$590 \pm 40$	$1080 \pm 50$

via the OH group; the presence of the remaining five deuterium atoms in the CH<sub>2</sub> group and the anthraquinone nucleus has no effect on the deactivation rate constant.

Besides being influenced by temperature and deuteration via the OH group, the T lifetime is affected by the nature of the solvent. A change of hexane for ethanol (Table III) increases the T and T- $d_6$  lifetimes approximately by a factor of 2.

For more definitive understanding of the nature of T and for interpretation of the results presented above, we have performed calculations of the potential energy surface of AQM in the ground and excited triplet states by the AM1 technique. The angle of OH-bond rotation about the CO bond (the dihedral angle of the COH plane and the anthraquinone nucleus plane) served as a reaction coordinate. Figure 8 demonstrates two types of the surfaces for the triplet state (2 and 2'). One of these surfaces (curve 2) was obtained with the anthraquinone core geometry fully optimized for the excited triplet state of AQM for which  $\theta = 8^\circ$ . The minimum of the potential energy surface corresponds to the "vertical" triplet state for which the singlet-triplet splitting energy is 0.91 eV. This value shows good agreement with the estimate. It is seen from Figure 1 that the position of the 0-0 band of the long-wave transition of AQM corresponds to ca. 1.8 eV, while the typical singlet-triplet splitting energy for the  $\pi\pi^*$  quinone states is<sup>29</sup> 6000 cm<sup>-1</sup> (0.75 eV). Hence, the triplet state should be higher than the ground state by approximately 1 eV. Besides the considered minimum corresponding to the "vertical" ( $\pi\pi^*$  in nature) triplet state, the potential energy surface showed another minimum corresponding to OH rotation by an angle of ca.  $130^\circ$ . Having optimized the anthraquinone core geometry, we obtained an even deeper minimum (by 0.4 eV) than that corresponding to the  $\pi\pi^*$  triplet (surface 2'). The second, deeper minimum corresponds exactly to the intermediate T appearing during the

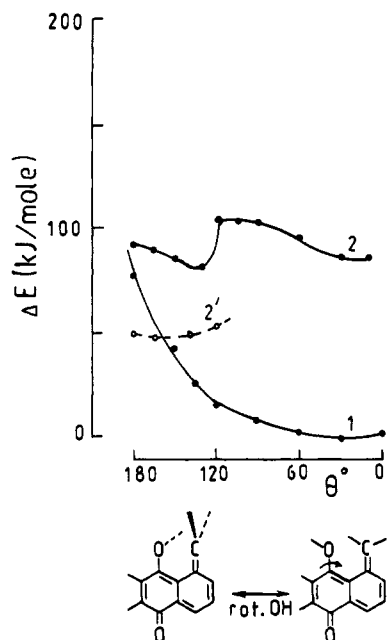


**Figure 8.** Potential energy surface of the ground state (1) and the lowest excited triplet state (2 and 2') of 9-acetoxy-1,10-anthraquinone-1-methide. The angle of OH-bond rotation about the CO bond is the reaction coordinate ( $\theta$ ). The length of the CH bond of the fragment  $\text{CH}_2$ , the OH-bond length, and their valence and dihedral angles were varied to minimize total energy. Curve 2 corresponds to the anthraquinone core geometry optimized for the plane  $^3\pi\pi^*$  (right minimum), and curve 2' corresponds to the anthraquinone core geometry optimized for the bi-radical triplet state (left minimum).

**Table IV.** CNDO Calculations for the Positions of Maxima ( $\nu$ ) and Oscillator Strengths ( $f$ ) of Transitions in Triplet-Triplet Absorption Spectra of the "Vertical" Triplet  $^3\pi\pi^*$  and  $\sigma,\pi$ -Biradical T

$^3\pi\pi^*$		T	
$\nu$ , $\text{cm}^{-1}$	$f$	$\nu$ , $\text{cm}^{-1}$	$f$
25 100	0.03	30 300	0.42
32 300	0.02	36 700	0.02
33 800	0.06	36 900	0.21
37 900	0.11	46 000	0.19
39 600	0.47		

hydrogen-atom transfer in the triplet AQ state. In this intermediate, one of the unpaired electrons is almost completely localized on the methylene group carbon atom (on the  $\sigma$ -orbital). The methide group plane of T is practically perpendicular to the plane of the anthraquinone nucleus. Hence, T is a triplet  $\sigma,\pi$ -biradical with twisted geometry. Intersystem crossing between states with different symmetries are known to have high rate constants.<sup>26a</sup> This explains the short lifetime of T (ca. 1  $\mu\text{s}$ ).

We have performed CNDO calculations of T-T absorption spectra of  $\pi\pi^*$  and T triplet states, including ca. 200 singly excited configurations<sup>21,22</sup> (Table IV). It is seen that in the calculated absorption spectrum of  $^3\pi\pi^*$ , there are low-intensity transitions within 25 000–34 000  $\text{cm}^{-1}$  and an intensive transition at 40 000  $\text{cm}^{-1}$ . A similar spectrum of T shows intensive transitions at 37 000 and 30 300  $\text{cm}^{-1}$ . The experimental spectrum (Figure 3, curve 3) exhibits intensive long-wave transitions in the visible and near-ultraviolet spectral regions (22 700 and 26 300  $\text{cm}^{-1}$ ). However, the long-wave band position in the absorption spectrum of AQM, calculated with the same parameters, turned out to be shifted into the shortwave region by 3000  $\text{cm}^{-1}$  as compared to the experimental spectrum in hexane and by 4700  $\text{cm}^{-1}$  for the spectrum in ethanol. The shift of the calculated bands of T into the shortwave region compared to experimental transitions is ca. 4000  $\text{cm}^{-1}$  (see Table IV), which is close to the case of AQM. Such an overestimation of the transition energy seems to be connected with the parametrization of the method. In view of this overestimation, it is seen that the calculated spectrum of T

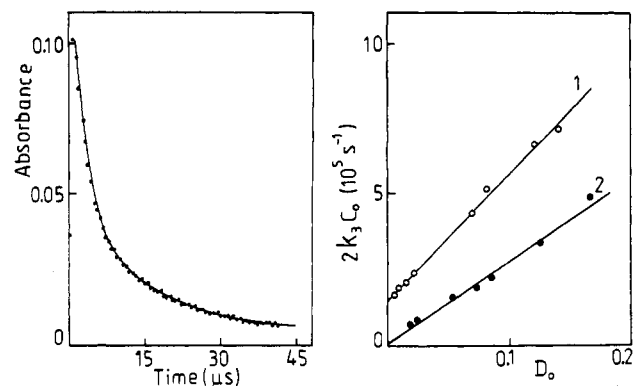


**Figure 9.** (A) Decay kinetics of the absorption of 9-deuteroxy-1,10-anthraquinone-1-methide (dots) and theoretical curve for the second-order reaction with the parameter obtained at the mean-square deviation minimum (solid curve). (B) Effective rate constant of the second-order reaction vs the initial concentration of AQM (1) or its deuterated analogue (2) in hexane at 206 K.

shows considerably better agreement with the experimental spectrum of the triplet intermediate than does the spectrum of  $^3\pi\pi^*$ . The absence of absorption of the intermediate in a range  $\lambda \geq 500$  nm is consistent with the calculated spectrum of T as well.

**Thermal Transfer of Hydrogen Atom.** It has been mentioned that in pulse experiments we detected both the accumulation of AQM from T and the decay of AQM due to its transformation to the initial quinone AQ. The thermal reaction was studied over a wide temperature range of 160–350 K in different solvents (Table V). At room temperature in all solvents under study, the AQM decay kinetic curve was described by exponential time dependence. Rate constants for intramolecular thermal transfer of hydrogen atom ( $k_2$ ) at 298 K are listed in Table V. However, with decreasing temperature in nonpolar solvents unable to form hydrogen bonds (hexane, toluene), the contribution of the second-order reaction becomes substantial. Thus in hexane at 206 K, we failed to exclude the contribution of the second-order reaction with initial AQM- $d_6$  concentration decreasing to  $10^{-6}$  mol/L. AQM concentration was varied by decreasing the intensity of the exciting laser pulse. The absorption decay kinetics of AQM- $d_6$  in hexane at 206 K are well described by the equation for the second-order reaction (Figure 9), with the effective rate constants derived from experimental data being linear with initial concentration of AQM- $d_6$  (Figure 9b). The kinetic curve for AQM is described by the sum of the first- and second-order reactions. Using the extinction coefficient of AQM<sup>8</sup> ( $10^4$  L/mol-cm), we have estimated the second-order rate constant ( $k_3$ ). In hexane at 206 K, it is  $(4.9 \pm 0.5) \times 10^9$  and  $(3.2 \pm 0.3) \times 10^9$  mol/L-s for AQM and AQM- $d_6$ , respectively. Theoretical estimation for the rate constant of the diffusion-controlled process by the formula  $k_{\text{diff}} = 8RT/3000\eta$  yields  $k_{\text{diff}} \approx 4 \times 10^9$  L/mol-s. The  $\eta$  value 1.15 cP was obtained by Arrhenius extrapolation of high-temperature data.<sup>30</sup>

Decreasing the laser pulse intensity, we succeeded in the exclusion of the second-order reaction in hexane for AQM at  $T \approx 190$  K and for AQM- $d_6$  at  $T \approx 220$  K. All over the temperature range under study, the temperature dependence of the rate constant of intramolecular transfer of H and D atoms is Arrhenius (Figure 10). Preexponentials for the rate constants of hydrogen- and deuterium-atom transfer in hexane coincide within experimental accuracy. The activation energy of the deuterium-transfer rate constant is higher by 7.5 kJ/mol and equals  $25.0 \pm 0.5$  kJ/mol. The kinetic isotope effect is strongly dependent on

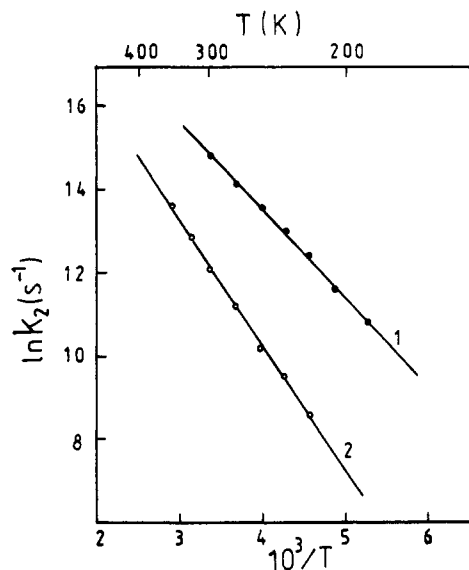
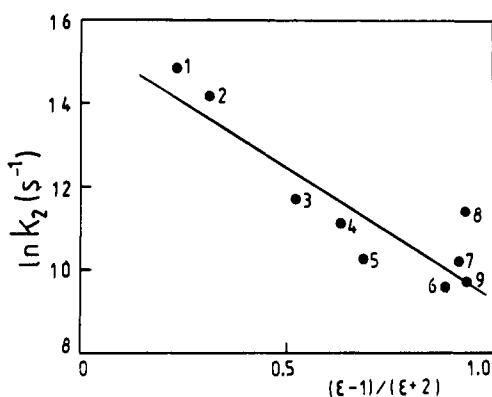
(30) Gornovskii, I. T.; Nazarenko, Yu. P.; Nekryag, E. F. *Concise Reference Book*; Naukova Dumka: Kiev, 1987; p 575.

(31) Gritsan, N. P.; Rogov, V. A.; Bazhin, N. M.; Russkikh, V. V.; Fokin, E. P. *Izv. Akad. Nauk SSSR, Ser. Khim.* **1980**, 89.

(32) It is assumed that the isotopic substitution of the H or D atom of the AQM hydroxy group for the D or H atom of the methanol hydroxy group proceeds much faster than does the intramolecular transfer reaction.

**Table V.** Rate Constants for the Intramolecular Transfer of Hydrogen Atom in 9-Hydroxy-1,10-anthraquinone-1-methide at 298 K ( $k_2$ ), Preexponential Factors ( $k_2^0$ ), and Activation Energies ( $E$ ) in Various Solvents

solvent	$k_2, \text{s}^{-1}$	$\log k_2^0, \text{s}^{-1}$	$E, \text{kJ/mol}$
hexane	$2.8 \times 10^6$	$9.5 \pm 0.1$	$17.5 \pm 0.5$
toluene	$1.5 \times 10^6$	$9.5 \pm 0.1$	$18.6 \pm 0.4$
diethyl ether	$1.4 \times 10^5$	$11.0 \pm 0.2$	$33.5 \pm 0.9$
ethyl acetate	$7.6 \times 10^4$	$11.1 \pm 0.2$	$33.6 \pm 1.0$
tetrahydrofuran	$2.8 \times 10^4$		
ethanol (abs)	$1.4 \times 10^4$	$10.2 \pm 0.2$	$34.3 \pm 1.1$
methanol (abs)	$2.7 \times 10^4$	$10.3 \pm 0.2$	$33.6 \pm 1.2$
acetonitrile	$9.1 \times 10^4$	$10.4 \pm 0.1$	$31.1 \pm 0.8$
dimethylformamide	$1.2 \times 10^4$		
ethanol (96%)	$1.2 \times 10^4$	$12.1 \pm 0.1$	$45.2 \pm 0.5$
2-propanol <sup>31</sup> (nonabs)	$1.6 \times 10^4$	$11.9 \pm 0.2$	$41.8 \pm 1.1$

**Figure 10.** Temperature dependence of the rate constant of intramolecular thermal transfer of hydrogen (1) and deuterium (2) atoms in hexane.**Figure 11.** Correlation of the hydrogen-atom transfer rate constant with the solvent dielectric coefficient function ( $\epsilon$ ).

temperature and increases from 16 at 298 K to 40 at 220 K.

The rate constant of the intramolecular transfer of hydrogen atom depends substantially on the nature of the solvent (Table V). The rate constant value of 298 K correlates well with the dielectric properties of a solvent (Figure 11). However, this is not the case for the activation energy. In nonpolar solvents unable to form hydrogen bonds, the activation energy is quite low, ca. 18 kJ/mol. In other thoroughly dehydrated solvents, including alcohols, it is 31–34 kJ/mol. In water-containing alcohols, the activation energy is considerably higher, 42–45 kJ/mol (Table V).

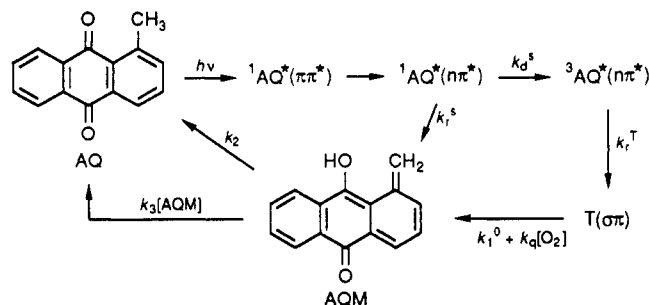
**Table VI.** Dependence of the Rate Constant of Thermal Migration ( $k_2$ ) of Hydrogen and Deuterium Atoms in Methanol at 298 K on Isotopic Substitution in the Methylene Group<sup>32</sup>

methide	$k_2^H, \text{s}^{-1}$	$k_2^D, \text{s}^{-1}$	$k_2^H/k_2^D$
$\text{CH}_2$	$2.7 \times 10^4$	$1.1 \times 10^4$	2.5
$\text{CD}_2$	$1.5 \times 10^4$	$1.6 \times 10^3$	9.4

The influence of the isotopic substitution in OH and  $\text{CH}_2$  groups on the rate constant turned out to be complex. The rate constant depends on isotope distribution in the OH group, as well as in the  $\text{CH}_2$  group (Table VI).

### Conclusion

Thus, the process of photochromic transformations of 1-methylantraquinone and its deuterated analogue can be presented by the following quite complex scheme:



Photochemical migration of hydrogen (or deuterium) atom occurs in both singlet and triplet  $n\pi^*$  states. The migration rate constant of hydrogen atom in the singlet state at  $T \lesssim 200$  K is independent of temperature and equals ca.  $10^{11} \text{ s}^{-1}$ . Hydrogen-atom phototransfer, in this case, can be treated as quantum tunnelling. The phototransfer of deuterium atom in the excited singlet state is thermally activated for all studied temperatures (120–340 K).

The rate constants of the phototransfer of hydrogen and deuterium atoms in the excited triplet state  $n\pi^*$  are at room temperature  $3 \times 10^{10} \text{ s}^{-1}$  and  $10^{10} \text{ s}^{-1}$ , respectively. A temperature decrease to ca. 200 K results in a decreased phototransfer rate constant, and the kinetic isotope effect is temperature independent and equals  $3.0 \pm 0.1$ . The short-lived triplet intermediate formed during the migration of hydrogen (or deuterium) atom in the  $3n\pi^*$  state has a structure of a triplet  $\sigma, \pi$ -biradical. The lifetime of this intermediate depends on temperature, solvent nature, and deuteration of the hydroxy group.

The enol AQM recovery to the initial quinone AQ can proceed in two ways: as an intramolecular process in the course of thermal migration of H or D atom, and by a second-order reaction. The bimolecular reaction appears to involve the transfer of two hydrogen (or deuterium) atoms in a collision complex of two AQM molecules. The rate constant of a second-order reaction in nonpolar aprotic solvents is close to the diffusion limit. No bimolecular process has been detected in polar solvents.

The rate constant of the intramolecular thermal transfer of hydrogen atom depends essentially on temperature, solvent nature, and deuteration of both hydroxy and methylene groups. No deviation of temperature dependence of the rate constants from Arrhenius curves has been observed. Isotopic substitution in the methyl group leads to an appreciable increase in the activation energy of the migration and has practically no influence on the preexponential factor.

**Acknowledgment.** The authors express their thanks to Professor N. M. Bazhin for valuable discussions and to Dr. A. A. Voityuk and Dr. A. A. Bliznyuk for making it possible for us to perform calculations with use of the MNDO-85 program.

**Registry No.** AQ, 954-07-4; AQ- $d_6$ , 134906-43-7; AQM, 71356-50-8; AQM- $d_6$ , 134938-22-0; D<sub>2</sub>, 7782-39-0; *o*-(*o*-toluyl)benzoic acid, 7111-77-5; toluene- $d_8$ , 2037-26-5; piperylene, 504-60-9.